HHS Public Access

Author manuscript

Clin Cancer Res. Author manuscript; available in PMC 2020 February 01.

Published in final edited form as:

Clin Cancer Res. 2019 February 01; 25(3): 1036–1049. doi:10.1158/1078-0432.CCR-18-0706.

Targeting PIM Kinase with PD1 inhibition Improves Immunotherapeutic Anti-Tumor T Cell Response

Shilpak Chatterjee[#1], **Paramita Chakraborty**[#1], **Anusara Daenthanasanmak**[2], **Supinya Iamsawat**[2], **Gabriela Andrejeva**[3], **Libia A Luevano**[4], **Melissa Wolf**[3], **Uday Baliga**[5], **Carsten Krieg**[2], **Craig C. Beeson**[6], **Meenal Mehrotra**[5], **Elizabeth G. Hill**[7], **Jeffery C. Rathmell**[3], **Xue-Zhong Yu**[2], **Andrew S. Kraft**[4], and **Shikhar Mehrotra**[*,1]

[1]Department of Surgery, Hollings Cancer Center, Medical University of South Carolina, Charleston, 29425

[2]Department of Microbiology & Immunology, Hollings Cancer Center, Medical University of South Carolina, Charleston, 29425

[3]Department of Pathology, Microbiology and Immunology, Vanderbilt University Medical Center, Nashville, TN 37232

[4]Department of University of Arizona Cancer Center, University of Arizona, Tucson, AZ, 85724.

[5]Department of Pathology & Laboratory Medicine, Hollings Cancer Center, Medical University of South Carolina, Charleston, 29425

[6]Department of Pharmaceutical and Biomedical Sciences, Hollings Cancer Center, Medical University of South Carolina, Charleston, 29425

[7]Department of Public Health, Hollings Cancer Center, Medical University of South Carolina, Charleston, 29425

[#] These authors contributed equally to this work.

Abstract

Purpose: Adoptive T cell therapy (ACT) of cancer, which involves the infusion of *ex vivo* engineered tumor epitope reactive autologous T cells into the tumor-bearing host, is a potential treatment modality for cancer. However, the durable anti-tumor response following ACT is hampered either by loss of effector function or survival of the anti-tumor T cells. Therefore, strategies to improve the persistence and sustain the effector function of the anti-tumor T cells are of immense importance. Given the role of metabolism in determining the therapeutic efficacy of T cells, we hypothesize that inhibition of PIM kinases, a family of serine/threonine kinase that promote cell cycle transition, cell growth, and regulate mTORC1 activity, can improve the potency of T cells in controlling tumor.

[*]*Corresponding Author*: Shikhar Mehrotra, Ph.D., Department of Surgery, Hollings Cancer Center (HO 512H), Medical University of South Carolina, 86 Jonathan Lucas Street, Charleston, SC 29425, USA, Phone: 843-792-9195; FAX: 843-792-2556, mehrotr@musc.edu.

Conflicts of Interest: The authors declare no potential conflicts of interest.

Experimental design: The role of PIM kinases in T cells was studies either by genetic ablation ($PIM1^{-/-}PIM2^{-/-}PIM3^{-/-}$) or its pharmacological inhibition (pan-PIM kinase inhibitor, PimKi). Subcutaneous murine melanoma B16 was established subcutaneously and treated by transferring tumor epitope gp100 reactive T cells along with treatment regimen that involved inhibiting PIM kinases, anti-PD1 or both.

Results: With inhibition of PIM kinases, T cells had significant reduction in their uptake of glucose, and upregulated expression of memory-associated genes that inversely correlate with glycolysis. Additionally, the expression of CD38, which negatively regulates the metabolic fitness of the T cells, was also reduced in PimKi-treated cells. Importantly, the efficacy of anti-tumor T cell therapy was markedly improved by inhibiting PIM kinases in tumor-bearing mice receiving ACT, and further enhanced by adding anti-PD1 antibody to this combination.

Conclusion: The present study highlights the potential therapeutic significance of combinatorial strategies where ACT and inhhibition of signaling kinase with check-point inhibition could improve tumor control.

Keywords

Adoptive T cell therapy; metabolism; PIM kinase; melanoma

INTRODUCTION

Harnessing the cytotoxic ability of T cells against tumor is a promising approach to devise effective T cell-based immunotherapy of cancer (1,2). Extensive studies have focused on optimizing the culture conditions for expanding tumor epitope-specific T cells. One of the important intrinsic parameters driving T cell differentiation and function is their metabolic commitment (3). It has been shown that dependence on glycolysis regulates the effector response of the T cells (e.g., IFNγ production) and leads to the generation of terminal effector T cells (4–6). Similarly, reliance on oxidative phosphorylation (OXPHOS) potentiates T cell memory response with improved persistence (7–9). Therefore, approaches to reinforce the differentiation of T cells to central memory phenotype (Tcm) have been successful by interfering with glycolytic activity of T cells either by blocking mTOR, AKT, or glycolytic pathway enzymes (6,10–17). Another strategy to increase the therapeutic efficacy of T cells for ACT is to reprogram the expanding T cells towards ‘stem cell-like memory’ (Tscm) phenotype (18–21). However, maintaining Tcm or Tscm phenotype in a tumor-bearing host has remained a challenge. Thus, understanding the mechanisms that lead to generation of stable anti-tumor Tcm phenotype *in vivo* has high translational potential to improve the quality of ACT.

PIM proteins are members of a family of short-lived, evolutionary conserved serine/threonine kinases comprised of three isoforms (PIM1, PIM2 and PIM3) that act downstream of cytokine receptors and are critical for various aspects of cellular processes including signal transduction, cell cycle progression, apoptosis, and cell metabolism (22). It has been shown that PIM kinases can promote the activity of mTOR and thus regulate cell growth and protein synthesis in various cancer types (23). Our data suggests that T cells obtained from triple PIM isoform knock out (TKO) mice exhibit low glycolytic activity, as evident by the

lower glucose levels and reduced mTOR activity when compared to WT controls. Importantly, no significant difference in T cell activation or proliferation was detected in TKO vs. WT T cells. Similar observations were obtained when T cells were activated in the presence of the pan-PIM kinase inhibitor (PimKi) AZD1208. Moreover, PIM kinase inhibition in T cells led to higher Foxo1 activity, which translated to a T central memory phenotype (T_{CM}, $CD44^{+}CD62L^{+}$) when compared with the control (vehicle-treated) T cells. Next, given the role of PIM kinases in down-modulating *MYC,(24)* which also controls PD1 expression (25,26), we assessed if combining anti-**P**D1 + pan-**P**IM **i**nhibitor + adoptive transfer of **T** cells (triple combination therapy, PPiT) could improve tumor response. We observed that when AZD1208 was administered with anti-PD1 antibody and tumor reactive T cells, there was long-term tumor control. Thus, we propose that targeting Pim kinase along with checkpoint blockade and adoptive T cell therapy offers potent tumor control.

Materials and Methods:

Mice

C57BL/6, B6-Thy1.1 (B6.PL-*Thy1*^{a}/CyJ) and pMel mice were obtained from Jackson Laboratory (Bar Harbor, ME). $PIM1^{-/-}PIM2^{-/-}PIM3^{-/-}$ mice (**t**riple **k**nock **o**ut or TKO mice) were obtained in collaboration with Andrew S. Kraft, University of Arizona. Animals were maintained in pathogen-free facilities and experimental procedures were approved by Institutional Animal Care and Use Committees of Medical University of South Carolina, Charleston.

Reagents and cell lines

Penicillin, streptomycin, glucose-free RPMI-1640, and Iscove's Modified Dulbecco's Medium (IMDM) were purchased from Life Technologies, Grand Island, NY. FBS was procured from Atlanta Biologicals, Atlanta. $hgp100_{25–33}$ peptide (KVPRNQDW) peptide was purchased from GenScript (Piscataway, NJ). Recombinant IL2 (rIL2) was procured from NCI, Biological Resources Branch. Fluorochrome conjugated anti-mouse CD8 (53–6.7), CD71 (RI7217), CD25 (PC61), CD69 (H1.2F3), CD44 (IM7), CD62L (MEL-14), Sca1 (D7), CD38 (90), PD1 (RPM1–30), IFN-γ (XMG1.2), IL-17a (TC11–18H10.1), CXCR3 (CXCR3–173) and anti-human CD8 (SK1), CD44 (IM7), CD62L (DREG-56), CD28 (CD28.2), CD27 (M-T271, PD1 (NAT105 were purchased from Biolegend, San Diego, CA. Anti-mouse Vβ13 (MR12–3) was procured from BD Biosciences, San Jose, CA. Anti-human Vβ12 was from Thermo Scientific (Rockford, IL). Anti-mouse pS6 conjugated with Alexa647, pAkt (S473) conjugated with PE and pFoxo1 (S256) were purchased from Cell Signaling Technology, Danvers, MA. Anti-mouse PD1 (RMP1–14), CD3 (145–2C11), and CD28 (37.51) were purchased from BioXcell, West Lebanon, NH. B16-F10 melanoma (Cat # CRL-6475) was obtained from ATCC, Manassas, VA and 624-MEL from Dr. Michael Nishimura (Loyola University). PBMCs from healthy donors were obtained from a commercial vendor, Research Blood Components, LLC, after institutional approval by the Human Investigation Review Board.

Cell Culture

Splenocytes from either TKO or WT (FvB) mice were activated with plate-bound anti-CD3 (2 μg/ml) and anti-CD28 (2 μg/ml) in presence of rIL2 (100 U/ml) for three days. In some cases, splenocytes from pMel mice were activated using $hgp100_{25–33}$ peptide (KVPRNQDW, 1μg/ml) either in presence of AZD1208 (3 μM) or vehicle (DMSO) for three days. rIL2 (100U/ml) was added during T cell activation. Complete IMDM media supplemented with 10% FCS, 4 mM L-glutamine, 100 U/ml penicillin, 100 μg/ml streptomycin, 55 μM beta-mercaptoethanol was used for T cell culture. Purified $CD4^+$ T cells were differentiated to either Th1 or Th17 type according to the protocol published recently (27).

Adoptive T cell protocol

Mouse melanoma tumor (B16-F10) and human melanoma (624-MEL) were maintained *in vitro* in complete IMDM. B16F10-ova (0.25×10^6) or 624-MEL (2.5×10^6) were injected subcutaneously (*s.c.*) into the left flank of C57BL/6 or NSG-A2 mice, respectively. On day 6 following B16-F10 cell inoculation, the C57BL/6 recipient mice were injected intraperitoneally (i.p.) with cyclophosphamide (CTX) at 4 mg/mice. After 24 h of CTX injection, tumor-bearing C57BL/6 were either kept untreated or adoptively transferred with three–day-activated pMel cells (1×10^6/mouse). For xenograft tumor experiments, 15 days *s.c.*-established 624-MEL in NSG-A2 mice were either kept untreated or treated with three-day-activated $CD4^+V\beta12^+$ (h3T) T cells (0.5×10^6/mouse). Recipient mice were given IL2 (50,000 U/mouse; i.p) for 3 consecutive days after ACT. In some cases, following ACT, recipient mice were either kept untreated or injected (i.p) with vehicle (methyl acetate), AZD1208 (15 mg/kg of body weight), anti-PD1 Ab (200 μg/mouse), or both AZD1208 and anti-PD1 Ab. Both AZD1208 and anti-PD1 Ab was given every other day until day 21.

Flow cytometry

Detailed protocol for staining of cell surface molecules and intracellular proteins has been described earlier (27). Samples were acquired on LSRFortessa and analysed with FlowJo software (Tree Star, OR).

Real-time quantitative-PCR

Total RNA was isolated from pellets of the indicated T cell subsets (2×10^6 cells) using Trizol reagent (Life Technologies, Grand Island, NY). cDNA was generated from 1 μg total RNA using iScript cDNA Synthesis Kit (BioRad, Hercules, CA). SYBR Green incorporation quantitative real-time PCR was performed using a SYBR Green mix (Biorad, Hercules, CA) in the CFX96 Detection System (BioRad, Hercules, CA).

Activation-induced T cell death

Three-day-activated T cells from either WT or TKO mice were either left untreated or re-stimulated overnight with plate bound anti-CD3 (2 μg/ml). Apoptosis was measured by Annexin V (BD Biosciences, San Jose, CA) vs. 7AAD staining according to the manufacturer's protocol, followed by flow cytometry. Data were analysed with FlowJo software (Tree Star, OR).

Glucose uptake, oxygen consumption and glycolytic flux

Glucose uptake by activated T cells were determined by incubating cells with 100 μM 2NBDG (Cayman Chemical, Ann Arbor, MI) for 30 minutes before measuring fluorescence by flow cytometry. Extracellular acidification rate (ECAR) was evaluated as described earlier (27).

Foxo1 activity assay

Using equal amounts of nuclear protein extracted by NE-PER Nuclear and Cytoplasmic Extraction Reagents (Thermo Fisher Scientific, Waltham, MA), Foxo1 activity (FKHR transcription Factor Assay Kit, Active Motif, Carlsbad, CA) was determined as per manufacturer's protocol.

Statistical analysis

All data reported are the arithmetic mean from three independent experiments performed in triplicate ± standard deviation (SD) unless stated otherwise. The unpaired Student's *t*-test was used to evaluate the significance of differences observed between groups, accepting $p < 0.05$ as a threshold of significance. Data analyses were performed using the Prism software (GraphPad, San Diego, CA). For tumor experiments, all analyses were performed using R version 3.2.3 and SAS version 9.4. Time-to-sacrifice was defined as the number of days from treatment to euthanasia (tumor size ≥ 400 mm^2 or other criteria for sacrifice met). Time-to-sacrifice values for animals not meeting euthanasia criteria at the end of the experiment were right-censored. Kaplan-Meier (KM) curves were constructed for each treatment group, and comparisons relative to control were performed using log-rank tests. Because KM curves frequently overlapped, curves were shifted slightly to facilitate visualization. Tumor size at each time point was measured relative to tumor size at treatment initiation to adjust for differences in tumor size at baseline between animals. We transformed resulting fold-change (FC) values using a log base 2 transformation to achieve approximate normality, evaluated using histograms and quantile-quantile plots. To facilitate transformation, we added 0.5 to tumor sizes of 0 mm^2. Using maximum likelihood, we fit linear mixed effects regression models of log_2FC as a function of experimental group, time (as a continuous variable), group-by-time interaction and mouse-specific random effects to account for the correlation among measures obtained from the same animal over time. We evaluated the functional form of time in each model, and considered non-linear transformations as appropriate based on fractional polynomials (28). Group comparisons were performed using model-based linear contrasts.

RESULTS

Inhibition of PIM kinases in T cells reduces their glycolytic activity

Since different T cell subsets (i.e., effector, memory, or regulatory) have been shown to exhibit unique metabolic commitment (29), we determined the metabolic phenotype of T cells in the absence of PIM expression. We observed that Pim TKO T cells significantly reduced their ability to uptake fluorescent glucose (2-NBDG, Fig. 1A), which could be due to the reduced expression of Glut1 on activated TKO T cells as compared to WT T cells

(Fig. 1B). To further interrogate whether absence of PIM kinases in T cells affects glycolysis, we evaluated extracellular acidification rate (ECAR), a measure of lactate production by aerobic glycolysis, in activated TKO and WT T cells using a metabolic flux analyzer. As shown in Fig. 1C, following the addition of glucose, TKO T cells exhibited a decreased ECAR value as compared to WT T cells, indicating that the ability of the TKO T cells to metabolize glucose through glycolysis is lower as compared to WT T cells.

To further determine whether reduced ECAR in TKO T cells was due to differential expression of key enzymes involved in the glycolytic pathway, we evaluated the transcript levels of various glycolytic enzymes using qPCR. Our data indicates that the transcript level of various glycolysis-associated genes was significantly downregulated in TKO T cells as compared to WT T cells (Fig. 1D). In addition to decreased glycolysis, deletion of PIM kinases in T cells also reduced the surface expression of transferrin receptor, CD71, which correlates positively with the glycolytic activity of these T cells (Fig. 1E). Since glycolysis positively corelates with the activation of mTOR, we next evaluated the phosphorylation of ribosomal protein S6 (pS6), a downstream target of mTOR, in WT and TKO T cells. We observed that WT T cells had a higher level of phosphorylated S6 as compared to TKO T cells (Fig. 1F). These data together imply that PIM kinases are involved in glycolytic commitment of T cells.

PIM kinase-deficient T cells exhibit increased T_{CM} phenotpe and reduced reactive oxygen species (ROS) generation

Since the glucose requirement is a key determinant of the IFNγ signature of T cells (5), we next determined if reduced glycolysis in TKO T cells affects the cytokine signature. Analysis of effector cytokines in activated T cells showed reduced IFNγ secretion by TKO T cells compared to WT T cells (Fig. 2A). Similarly, TKO T cells differentiated *in vitro* to either Th1 or Th17 cells exhibited reduced signature cytokine secretion compared to WT T cells (Fig. 2B).

Next, to determine if the reduced cytokine response exhibited by TKO T cells is due to lack of proper activation or differentiation, we compared the phenotype of activated WT and TKO T cells after three days. We observed that both WT and TKO T cell populations had similar level of CD25 and CD69 expression (Fig. 2C), indicating an equal degree of activation. However, we noticed that compared to WT T cells, the majority of the TKO T cells exhibited the $CD62L^{+}CD44^{+}$ phenotype (≈ 60% vs. 40%, Fig. 2D). This was also accompanied by increased expression of stem cell antigen (Sca1) on this Tcm fraction in TKO T cells (Fig. 2E). Thus, inhibition of PIM kinases results in an increased Tcm fraction with a stem cell phenotype. Various negative co-stimulatory molecules (PD1 and CD38) that have been shown to dampen the effector response of the T cells at the tumor site were markedly reduced on TKO T cells as compared to WT T cells (Fig. 2F and 2G). T cell receptor (TCR) restimulation results in ROS secretion that has been shown to be important for initial proliferation of the T cells (30). Thus, we examined if there is any difference in ROS accumulation between WT and TKO T cells. Our data shows that PIM TKO T cells secreted lower levels of ROS species H_2O_2 (measured using DCFDA) and reactive nitrogen species (RNS, measured using DAF; Fig. 2H and 2I). The anti-oxidant genes (such as

catalase, superoxide dismutase, thioredoxin; measured using qPCR) were also found to be elevated in PIM TKO T cells (Fig. 2J). Since excessive ROS/RNS accumulation upon chronic TCR activation leads to activation-induced cell death (AICD), we determined if there are any differences in susceptibility to AICD between the WT and PIM TKO T cells. Our data shows that TCR activated PIM TKO T cells, upon TCR restimulation, exhibited reduced cell death (as measured by Annexin V) as compared to WT T cells (Fig. 2K). Thus, loss of PIM in primary T cells seems to correlate with reduced ROS/RNS and a lesser degree of cell death. It should be noted that data showing reduced ROS in primary T cells is different from what we reported earlier for PIM TKO mouse embryonic fibroblasts (MEFs) (31), (Fig. 2L). This set of data gave us an impetus to target PIMs along with ACT for tumor control, since on one hand, PIM inhibition could lead to depletion of Nrf2 and ROS-mediated tumor lysis, while on the other hand, T cells may exhibit the opposite phenotype—reduced ROS/cell death.

Further, the RNA sequence analysis using the TCR activated WT and TKO derived T cells (Supplementary Fig. 1) also revealed inhibition of the glycolysis and glycogen pathway genes as *Eno* (enolase), *Pygl* (glycogen phosphorylase), *Gbe* (glycogen branching enzyme). While enolase has been shown to regulate regulatory T cells (32), the glycogen metabolism pathway genes primarily indicate declined cellular glycogen content and decreased rates of glycogenolysis or glycogenesis. The expression of bone morphogenetic protein family proteins and receptors (members of the TGF-beta superfamily) was decreased in TKO T cells as compared to WT counterpart. The expression of *Bmp7* has also been shown to directly correlate with B cell apoptosis (35). TKO T cells showed increased expression of *Cadm1* (cell adhesion molecule 1), *Bcl2a1 (*Bcl-2-related protein A1), *Tnfsf4* (OX40L), and *Sell* (CD62L) which are known to promote lymphocyte adhesion, migration, survival (36–38). Expression of several solute transporters as *Slc12a2*, *Slc25a10* (malate transporter on mitochondrial membrane), *Slc15a3*, and *Slc7a11* (cystine/glutamate transporter, xCT) were increased in TKO T cells. Several mitochondrial transporters or electron transport chain components as *Nudt1* (Nudix hydrolase 1), *mt-ND1*, *mt-CytB*, *Timm10*, and *Timm50* were also elevated in TKO T cells. While *Nudt1* encodes protein that hydrolyzes oxidized purine nucleoside triphosphates to facilitate DNA repair (39), *mt-ND1* and *mt-CytB* are important part of the electron transport chain. Similarly, *Timm50* expression prevents the release of cytochrome c and apoptosis. Thus, deletion of PIM modulated the pathways that led to improved survival and function of the T cells.

Pharmacological inhibition of PIM kinases decreases T cell metabolism

We next determined the biologic outcome of pharmacological inihibition of PIM kinases in T cells, specifically whether using AZD1208 (40) treatment would produce a similar metabolic and functional phenotype as observed with TKO T cells. Our data indicates that, similar to TKO T cells, inhibition of PIM kinases by AZD1208 reduced the ability of T cells to uptake fluorescent glucose analogue (2NBDG, Fig. 3A), which further correlates with the reduced glycolysis rate of the cells as measured by ECAR (Fig. 3B). In both cases (Fig. 1C and 3B) only basal glycolysis rate was found to be significantly different between the groups whereas the glycolytic capacity (defined as the difference between ECAR following the injection of oligomycin and the basal ECAR reading) and glycolysis reserve (defined as the

difference in ECAR between the glucose and oligomycin injections) were comparable between the groups. Evaluation of intracellular metabolites futher confirmed that the inhibition of PIM kinases in T cells markedly reduces their glycolytic activity. The intracellular level of lactate, the terminal metabolite of aerobic glycolysis, was markedly reduced in T cells treated with AZD1208 as compared to vehicle-treated group (Fig 3C). Moreover, the expression of CD71 and phosphorylation of ribosomal protein S6 are substantially reduced in T cells treated with PimKi (Fig. 3D and 3E), indicating that AZD1208 treatment produces a comparable effect to genetic ablation of PIM kinases in altering the glycolytic comitment of the T cells.

We next determined the functional phenotype of the T cells activated in presence of AZD1208, and found that its treatment substantially increased the percentage T_{CM} cells ($CD44^{+}CD62L^{+}$, Fig. 3F). The expression of chemokine receptor CCR7, a key molecule on Tcm cells (41), was also enhanced in T cells activated in presence of AZD1208 (Fig 3G). However, no significant difference in the activation status of the T cells, as determined by the expression of CD25 and CD69, was observed between vehicle vs. AZD1208 treatment groups (Supplementary Fig. 2A), implying that Tcm phenotype was not related to reduced activation. Moreover, similar to TKO T cells, AZD1208-treated T cells also exhibited marked reduction in the surface expression of co-inhibitory molecule PD1 (Fig. 3H, *upper panel*), and ectonucleotidase CD38 (Fig. 3H, *lower panel*), which was recently shown to inversly correlate with anti-tumor T cell function (27).

Next, we compared the cytokine production between vehicle vs. AZD1208-treated T cells and observed that pharamacological blockade of PIM kinases substantially reduced the IFNγ and IL17 secretion from *in vitro* differentiated Th1 and Th17 cells respectively (Fig. 3I). The RNA sequence analysis also showed differences in similar metabolic pathway genes, and genes responsible for migration, proliferation and survival as was observed with TKO T cells (Supplementary Fig. 2B). These data together indicate that pharamacological blockade of PIM kinases using AZD1208 induced similar metabolic and functional phenotype of T cells to that observed for TKO T cells.

Reduced phosphorylation of Foxo1 in AZD1208-treated T cells

Given the increased expression of CD62L in AZD1208-treated T cells, we reasoned that the upstream transcription factor Foxo1, which regulates CD62L expression (42,43), should be activated. Since increased phosphorylation of Foxo1, mediated by Akt, leads to exclusion of this protein from the nucleus and reduction in its activity (44,45), we determined the phosphorylation levels of both Foxo and Akt. Our data shows that AZD1208-treated T cells indeed exhibit reduced phosphorylation of both Akt and Foxo1 (Fig. 4A and 4B).

Quantitative determination of the transcriptional acitivity of the Foxo1 (Fig. 4C) further correlated with the cofocal microscopy data (Fig. 4D), demonstrating that AZD1208 treatment significantly increases the transcriptional activity of Foxo1 in T cells. As increased transcriptional activity of Foxo1 has been shown to regulate the expression of various memory-associated molecules like Tcf7, Bcl6 and β-catenin, we next evaluated the expression of these molecules in T cells treated with AZD1208. We observed significant upregulation in the mRNA expression of both *Tcf7* (~2 fold) and *Bcl6* (~1.5 fold) in T cells

treated with AZD1208 as compared to the vehicle-treated group (Fig. 4E). This data demonstrates that PIM inhibition corresponds to the upregulation of memory and stemness phenotype, likely mediated by increased Foxo1 activity.

In order to determine if pan-PIM inhibitor AZD1208 pre-treated T cells would establish memory *in vivo*, we activated melanoma epitope gp100 reactive T cells derived from pMel TCR transgenic T cells with cognate antigen for three days either alone or in presence of AZD1208 and transferred them *i.v.* into $Rag1^{-/-}$ mice. After 25 days of initial transfer of T cell, the recipient mice were sub-cutaneously injected with murine melanoma B16-F10 cells. Then homeostatically proliferating transgenic T cells were tracked after 5 days of tumor injection in different lymphoid and non-lymphoid organs. We observed that pMel+AZD1208 T cells exhibited higher recall response to tumor challenge as compared to pMel control T cells, which was evident by its significantly increased expansion in each organ (Fig. 4F). Additionally, the AZD1208 treated pMel T cells tracked from the spleen of recipient mice also showed enhanced cytokine secretion upon restimulation, as compared to the untreated ones (Fig. 4G). This indicates that PIM kinase inhibition renders T cells with a functional memory phenotype.

PIM kinase inhibition leads to improved tumor control

Given that inhibition of glycolysis produces T cells with increased memory phenotype, which is crucial for exerting durable anti-tumor response (6), we determined if inhibition of PIM kinases will improve control of solid tumor. Thus, gp100 reactive T cells (from pMel TCR transgenic mouse) were pre-treated with PimKi, adoptively transferred to the C57BL/6 mice bearing subcutaneously established murine melanoma B16-F10, and tumor growth was monitored (Fig. 5A). A maintenance dose of AZD1208 was also administered twice weekly for three weeks after adoptive transfer, and groups of mice with ACT alone and inhibitor alone were used as controls. Our data demonstrates that PIM inhibition along with adoptively transferred T cells showed improved tumor control and survival as compared to the groups treated with ACT or inhibitor alone (Fig. 5B). However, the increased survival was short-lived – likely due to dimished effect of pharmacological inhibition with time.

The inhibition of PIM kinase during TCR-mediated activation of human T cells also conferred a phenotype similar to the one observed for murine TKO cells or for AZD1208-treated murine WT T cells. As shown in Fig. 5C, inhibition of PIM in human T cells resulted in increased Tcm phenotype as exhibited by the $CD44^{+}CD62L^{+}$ levels. Additionally, we found that despite TCR activation and proliferation, the human T cells maintained elevated expression of CD28 (Fig. 5D) and CD27 (Fig. 5E) when compared to the untreated T cells. Moreover, as observed in murine T cells, the human T cells activated in presence of AZD1208 also showed reduced expression of PD1 (Fig. 5F) and CD38 (Fig. 5G) as compared to those activated without it. Next, we analysed the metabolic phenotype of the human T cells treated with PimKi and found that similar to the murine T cells, inhibition of PIM kinases significantly reduced the ability of the human T cells to uptake fluorescent glucose (2-NBDG, Fig. 5H). This data indicates that, like in the mouse, inhibition of PIM kinases in human T cells hampered their glycolytic activity, which was further correlated

with the reduced phosphorylation of ribosomal protein S6 (pS6) in human T cells treated with AZD1208 (Fig. 5I).

To further evaluate whether ACT in the presence of PimKi is equally efficacious in controlling human tumors, we subcutaneously established HLA-A2$^+$ human melanoma 624MEL cells in NSG-A2 recipient mice. The h3T TCR trangenic mouse-derived human tyrosinase epitope-reactive T cells were used for adoptive transfer either alone or combined with AZD1208 treatment (Supplementary Fig. 3A). Our data shows that human tumors also showed the similar trend with slower growth and better survival in the mice that were treated with the combination of PimKi and tumor reactive T cells (Supplementary Fig. 3B, 3C*).* However, it seems that slow tumor growth was restricted to the three week duration when the maintenance does of PimKi was adminsitered (with *p* value being 0.0264 (d8), 0.001 (d15), 0.0006 (d17), 0.0006 (d20), 01692 (d26)). Thus, the strategy to combine PimKi with ACT could be beneficial for achieving tumor control in immunotherapy protcols, but may require a long-term pharmacological inhibition of PimK.

The combination AZD1208 treatment with anti-PD1 antibody further improves ACT

The murine B16F10 melanoma cell line is resistant to checkpoint blockade with antibodies targeting the PD-1 and/or CTLA-4 (cytotoxic T lymphocyte–associated protein 4) receptors (46,47). Therefore, strategies that could increase efficiacy of immune check-point blackade are needed. Since PimKi increased Tcm/Tscm phenotype, we hypothesized that a combinatorial approach using anti-**P**D1 + pan-**P**IM **i**nhibitor + adoptive transfer of **T** cells (triple combination therapy, PPiT) could improve monotherapy with anti-PD1 or ACT. Our experiments demonstrated that PPiT worked the best in controlling growth of established melanoma (Fig. 6A), and markedly enhanced the survival of tumor bearing mice (Fig. 6B). Importantly, the tumor growth was significanty lower when Pmel T cells were adminstered with PimKi with anti-PD1 (brown solid curve, PPiT group) as compared to PimKi alone (red solid curve). However, this reduced tumor growth in PPiT group was limited to the duration of PimKi administration, as the tumors grew back and reached to the size similar to one's observed in the group treated with T cells and AZD1208. The statistical analysis showed that as compared to Pmel group, PPiT group remained statistically significant (<0.0001) from day 8–32, where as in Pmel+AZD group the *p* values were 0.0685 (d8), 0.012 (d11), 0.0083 (d13), 0.0081 (d15), 0.0176 (d19), 0.0389 (d21), 0.2673 (d25), 0.5737 (d27, non significant), and 0.5859 (d32, non significant). Thus, it seems that the PPiT treated group did had a better overall tumor control as compared to pMel+AZD1208 group. This data indicates that adding AZD1208 throughout the anti-PD1 regimen could have potential clinical relevance for patients being treated with this antibody.

To determine if differences in T cell migration or persistence played a role in the enhanced tumor control observed with PPiT, we tracked the adoptively transferred T cells in the spleen, blood, and tumor site. A higher number of adoptively transferred gp100-reactive T cells were observed in mice that received triple combination (Fig. 6C). Importantly, for PPiT-treated mice, expression of PD1 (Fig. 6D) and CD38 (Fig. 6E) was reduced in T cells retrieved from the tumor site, but there was an increase in cytokine response (IFNγ, TNFα) along with granzyme B (Fig. 6F). We also observed that the expression of PD1 and CD38

was considerably lower on adoptively transferred T cells retrieved from the spleen or blood of tumor-bearing mice receiving PPiT (Fig. 6G and 6H). Moreover, the expression of CXCR3, which correlates with the improved migration of the anti-tumor T cells to the tumor site, was also elevated on the tumor epitope-specific T cells from spleen or blood of tumor-bearing mice receiving PPiT (Fig. 6I and 6J). It must be noted that the data in Fig. 6C-6I was generated when the tumor size in pMel+AZD and PPiT group were almost similar, since the last adminsitration of PimKi was about two or more weeks before the experimental endpoint, which would have resulted in the diminished PimK inhibition leading the tumor to grow after day 21 and masking the diffrences in phenotype and function of infiltrated T cells. However, the data does indicate that PIM inhibitor and anti-PD1 produced quantitative and qualitative changes in T cell phenotype that leads to long-lasting tumor control. Together, these results suggest that the PPiT strategy could be potentially tarnslated to clinics for targeting tumors where anti-PD1 therapy has not yielded durable anti-tumor control.

DISCUSSION

Studies in animal models indicate that adoptive transfer of long-lived, central memory T cells (T_{CM}) significantly improves their persistence and the therapeutic efficacy of adoptive immunotherapies. However, most adoptive cell transfer (ACT) trials use rapidly expanded T cells—either TCR- or chimeric antigen receptor-engineered or tumor infiltrating lymphocytes (TILs)—that are terminally differentiated and/or have an effector memory (T_{EM}) phenotype (1,48). These terminally differentiated T cells also exhibit negative co-stimulatory molecules (i.e. CTLA4, PD1, Tim-3) that correlate with T cell dysfunctionality or exhaustion and have limited life span *in vivo*, making them less likely to mediate clinical responses (49,50). Based on the promising results seen when using check-point blockade, it is important that the mechanisms underlying the resistance to these therapies are better understood and targeted for increasing the efficacy of tumor control across various tumor types (51–53). Thus, strategies that could potentiate anti-tumor immunotherapy are needed.

The three Pim kinases are members of a small family of serine/threonine kinases regulating several signaling pathways that are fundamental to cancer development and progression (54). It has been shown that similar to the rapamycin target TOR, the Pim kinases also contribute to the regulation of lymphocyte growth and proliferation (55). This study also showed that $PiM1^{-/-}PIM2^{-/-}$ T cells have increased sensitivity to rapamycin. Since rapamycin-mediated mTOR inhibition has been shown to increase the T cell memory response (13,56,57), we hypothesized that targeting PIM kinases could produce an even stronger T cell memory phenotype and thereby potentiate tumor control. We show here that combining PIM kinase inhibition with anti-PD1 antibody renders T cells with Tcm/Tscm phenotype, which is maintained *in vivo* and improves tumor control when this approach is used to treat poorly immunogenic murine melanoma B16-F10 tumors. Importantly, the TILs obtained from the tumors of groups that were treated with PIM inhibitor showed decreased expression of both CD38 and PD1. A recent study has shown that discrete chromatin states correlate with reprogrammability and surface protein expression profiles, where high CD38 expression was associated with non-reprogrammable $PD1^{hi}$ dysfunctional T cells within heterogeneous T cell populations (58). Reduced CD38 expression has also been shown to

result in increased levels of NAD^+ within the T cells, which renders anti-tumor T cells with a “metabolic fitness” and result in improved tumor control(27). Thus, maintaining high NAD^+ by blocking CD38 expression due to PIM inhibition may have also contributed to the improved tumor response and needs to be further investigated.

It has been shown that blocking T cell differentiation promotes the generation of Tscm cells with $CD44^{lo}CD62L^{hi}Sca\text{-}1^{hi}$ phenotype that exhibit enhanced anti-tumor capacity (20). However, we observed that inhibition of PIM kinase leads to enhanced Tscm phenotype without hampering T cell activation, which could be due to differences in phosphorylation status of its downstream substrates that are involved in cellular differentiation (59). To our knowledge, the synergy between adoptive T cell immunotherapy, check-point blockade, and a protein kinase inhibitor, reported in this study, to significantly increase tumor control has not been demonstrated earlier.

PIM kinase and Akt are the two pro-survival kinases that are commonly amplified in cancer (60), and they are also known to cross-talk (60). These oncogenic proteins are serine/threonine kinases that phosphorylate various substrates that control the cell cycle, cellular metabolism, proliferation, and survival (60). We observed that PimKi-treated T cells also exhibited reduced phosphorylation of Foxo, which is mediated by phosphorylated Akt (61). Foxo1 is required to maintain naive T cell homeostasis through the regulation of several genes crucially involved in T cell trafficking and survival (44). The Foxo subfamily of transcription factors also has a highly conserved role in the regulation of life span, cell cycle progression, apoptosis, glucose metabolism, and stress resistance, which works by integrating information pertaining to the abundance of nutrients, growth factors and stress signals (45). The increased nuclear retention of Foxo1 that correlates with its enhanced functional activity was likely responsible for the shift to a Tcm phenotype and higher levels of its downstream transcriptional target, i.e., CD62L (42). Systemic administration of PimKi in our approach could also have resulted in the continuous activity of Foxo1, which has recently been shown to be required for preventing anergy and maintaining the memory state of $CD8^+$ T cells (62).

Our data also suggests that PIM kinases positively regulate glycolysis in T cells and its inhibition leads to reduced glycolysis, increased persistence and enhanced tumor control. This data recapitualtes the previous striking observation that inhibition of glycolysis in T cells potentiates tumor control by increasing persistence and maintaining effector function *in vivo* (6). The systemic administration of pan-PIM inhibitor may also have metabolically modulated other endogenous lymphoid and myeloid cells of the tumor-bearing host. Inhibition of mTOR promotes dendritic cell (DC) activation and enhances T cell response upon vaccination (63). The improved performance of DCs in which mTOR has been inhibited is correlated with an extended lifespan following activation and a prolonged increase in expression of costimulatory molecules (63). A recent study has also shown that glucose-deprived GM-DCs demonstrate increased costimulatory molecule and IL12 expression, signals known to be important for the induction of T-cell proliferation and the acquisition of T cell effector function (64). Foxo1 also induces DC activity by regulating ICAM-1 and CCR7 (65) by binding to the CCR7 and ICAM-1 promoters, stimulating CCR7 and ICAM-1 transcriptional activity, and regulating their expression (65).

We observed that inhibition of PIM kinase does affect the human T cell survival and function. While there was an increase in Tcm phenotype, we also noticed reduced pFoxo, pAkt and enhanced Foxo activity in AZD1208-treated T cells *in vitro*. The FOXO binding site (TGTTTAC) and several FOXO target genes are conserved from worms to mammals, raising the possibility that the PIM mediated regulation of FOXO-dependent transcription may be conserved across species (66). We also noticed increased CD28, a positive co-stimulatory molecule that controls mitochondrial dynamics and metabolic fate of T cells (67). Thus, the likelihood of translating the PPiT strategy into patients is high, as this combination approach may have the potential to increase tumor control by metabolically altering T cells in the tumor microenvironment.

While our data demonstrates that PimKi-treated T cells have reduced pAkt, pFoxo, and pS6, there still could be various substrates that may be hypo-phosphorylated, causing differences in TCR signalling or metabolic signalling. Recently, the role of protein phosphorylation as a major switch mechanism for metabolic regulation has been discussed (68). Protein kinases phosphorylate a substrate, modulating its activity. While it seems simple, multiple kinases can phosphorylate the same substrates, mostly on different sites within the same protein. This could lead to a highly connected network of metabolic control points. Future studies will be needed to identify the differences in phosphorylation state of different PIM substrates within diverse immune cells. These findings could help us identify the specific signalling pathways that are altered by kinase inhibitors and contribute to tumor control.

While we do observe high levels of effector cytokines (IFNγ, TNFα), along with enhanced levels of the cytolytic molecule, granzyme B, and reduced T cell exhaustion in the AZD1208- or PPiT-treated tumor-bearing animals, the administration of AZD1208 alone did not produce significant tumor control; thus, it is likely that this agent may affect tumor or the microenvironment, making the tumor more susceptible to lysis by adoptively transferred T cells, which alone were also less effective, yet in contrast these cells had remarkably preserved effector function and stemness in the PPiT treatment group. Identifying targets of modulation within transferred or host immune cells when using the PPiT strategy will be important for designing future target specific trials. Similarly, elucidating the role of individual PIM isoforms in T cells would be required to refine this approach for boosting anti-tumor T cell effector and memory responses (69,70). Importantly, this study establishes that strategies that target tumor tissues and boost the host immune response have the potential for achieving long-term tumor control.

Supplementary Material

Refer to Web version on PubMed Central for supplementary material.

ACKNOWLEDGEMENT

Conception and design: SC, PC, SM. Development of methodology: SC, SM. *Acquisition of data (provided animals, acquired and managed patients, provided facilities, etc.):* SI, GA, LAL, MW, UB, CK, JCR, ASK. Analysis and interpretation of data (e.g., statistical analysis, biostatistics, computational analysis): SC, EH, GA, JCR, MM, CB, SM. Writing, review, and/or revision of the manuscript: SC, ASK, XY, SM. Administrative, technical, or material support (i.e., reporting or organizing data, constructing databases): SC, PC, CK, MM, XY, SM. Study supervision: SM. The authors sincerely acknowledge Michele Zacks at UACC for editing this manuscript.

Financial support: The work was supported in part by NIH grants R21CA137725, R01CA138930, and P01CA154778 to S.M. Support from Hollings Cancer Center Shared Resources (partly supported by P30 CA138313) at MUSC is also acknowledged. This study was supported by University of Arizona Cancer Center support grant P30CA023074, NIH award R01CA173200, and DOD award W81XWH-12–1-0560 (to A.S.K.)

REFERENCES

1. Yang JC, Rosenberg SA. Adoptive T-Cell Therapy for Cancer. Adv Immunol 2016;130:279–94 doi 10.1016/bs.ai.2015.12.006. [PubMed: 26923004]
2. Fesnak AD, June CH, Levine BL. Engineered T cells: the promise and challenges of cancer immunotherapy. Nat Rev Cancer 2016;16(9):566–81 doi 10.1038/nrc.2016.97. [PubMed: 27550819]
3. Sugiura A, Rathmell JC. Metabolic Barriers to T Cell Function in Tumors. J Immunol 2018;200(2): 400–7 doi 10.4049/jimmunol.1701041. [PubMed: 29311381]
4. Chang CH, Curtis JD, Maggi LB, Jr., Faubert B, Villarino AV, O'Sullivan D, et al. Posttranscriptional control of T cell effector function by aerobic glycolysis. Cell 2013;153(6):1239–51 doi 10.1016/j.cell.2013.05.016. [PubMed: 23746840]
5. Cham CM, Gajewski TF. Glucose availability regulates IFN-gamma production and p70S6 kinase activation in CD8+ effector T cells. J Immunol 2005;174(8):4670–7. [PubMed: 15814691]
6. Sukumar M, Liu J, Ji Y, Subramanian M, Crompton JG, Yu Z, et al. Inhibiting glycolytic metabolism enhances CD8+ T cell memory and antitumor function. J Clin Invest 2013;123(10): 4479–88 doi 10.1172/JCI69589. [PubMed: 24091329]
7. van der Windt GJ, Everts B, Chang CH, Curtis JD, Freitas TC, Amiel E, et al. Mitochondrial respiratory capacity is a critical regulator of CD8+ T cell memory development. Immunity 2012;36(1):68–78 doi 10.1016/j.immuni.2011.12.007. [PubMed: 22206904]
8. van der Windt GJ, Pearce EL. Metabolic switching and fuel choice during T-cell differentiation and memory development. Immunol Rev 2012;249(1):27–42 doi 10.1111/j.1600-065X.2012.01150.x. [PubMed: 22889213]
9. van der Windt GJ, O'Sullivan D, Everts B, Huang SC, Buck MD, Curtis JD, et al. CD8 memory T cells have a bioenergetic advantage that underlies their rapid recall ability. Proc Natl Acad Sci U S A 2013;110(35):14336–41 doi 10.1073/pnas.1221740110. [PubMed: 23940348]
10. Gattinoni L, Klebanoff CA, Restifo NP. Pharmacologic induction of CD8+ T cell memory: better living through chemistry. Sci Transl Med 2009;1(11):11ps2 doi 10.1126/scitranslmed.3000302.
11. Li Q, Rao R, Vazzana J, Goedegebuure P, Odunsi K, Gillanders W, et al. Regulating mammalian target of rapamycin to tune vaccination-induced CD8(+) T cell responses for tumor immunity. J Immunol 2012;188(7):3080–7 doi 10.4049/jimmunol.1103365. [PubMed: 22379028]
12. Li Q, Rao RR, Araki K, Pollizzi K, Odunsi K, Powell JD, et al. A central role for mTOR kinase in homeostatic proliferation induced CD8+ T cell memory and tumor immunity. Immunity 2011;34(4):541–53 doi 10.1016/j.immuni.2011.04.006. [PubMed: 21511183]
13. Srivastava RK, Utley A, Shrikant PA. Rapamycin: A rheostat for CD8(+) T-cell-mediated tumor therapy. Oncoimmunology 2012;1(7):1189–90 doi 10.4161/onci.20663. [PubMed: 23170275]
14. Crompton JG, Sukumar M, Restifo NP. Targeting Akt in cell transfer immunotherapy for cancer. Oncoimmunology 2016;5(9):e1014776 doi 10.1080/2162402X.2015.1014776. [PubMed: 27757294]
15. Crompton JG, Sukumar M, Roychoudhuri R, Clever D, Gros A, Eil RL, et al. Akt inhibition enhances expansion of potent tumor-specific lymphocytes with memory cell characteristics. Cancer Res 2015;75(2):296–305 doi 10.1158/0008-5472.CAN-14-2277. [PubMed: 25432172]
16. Klebanoff CA, Crompton JG, Leonardi AJ, Yamamoto TN, Chandran SS, Eil RL, et al. Inhibition of AKT signaling uncouples T cell differentiation from expansion for receptor-engineered adoptive immunotherapy. JCI Insight 2017;2(23) doi 10.1172/jci.insight.95103.
17. Sukumar M, Roychoudhuri R, Restifo NP. Nutrient Competition: A New Axis of Tumor Immunosuppression. Cell 2015;162(6):1206–8 doi 10.1016/j.cell.2015.08.064. [PubMed: 26359979]

18. Gattinoni L, Klebanoff CA, Restifo NP. Paths to stemness: building the ultimate antitumour T cell. Nat Rev Cancer 2012;12(10):671–84 doi 10.1038/nrc3322. [PubMed: 22996603]
19. Gattinoni L, Speiser DE, Lichterfeld M, Bonini C. T memory stem cells in health and disease. Nat Med 2017;23(1):18–27 doi 10.1038/nm.4241. [PubMed: 28060797]
20. Gattinoni L, Zhong XS, Palmer DC, Ji Y, Hinrichs CS, Yu Z, et al. Wnt signaling arrests effector T cell differentiation and generates CD8+ memory stem cells. Nat Med 2009;15(7):808–13 doi 10.1038/nm.1982. [PubMed: 19525962]
21. Gattinoni L, Lugli E, Ji Y, Pos Z, Paulos CM, Quigley MF, et al. A human memory T cell subset with stem cell-like properties. Nat Med 2011;17(10):1290–7 doi 10.1038/nm.2446. [PubMed: 21926977]
22. Santio NM, Koskinen PJ. PIM kinases: From survival factors to regulators of cell motility. Int J Biochem Cell Biol 2017;93:74–85 doi 10.1016/j.biocel.2017.10.016. [PubMed: 29108877]
23. Rebello RJ, Huglo AV, Furic L. PIM activity in tumours: A key node of therapy resistance. Adv Biol Regul 2017 doi 10.1016/j.jbior.2017.10.010.
24. Zhang Y, Wang Z, Li X, Magnuson NS. Pim kinase-dependent inhibition of c-Myc degradation. Oncogene 2008;27(35):4809–19 doi 10.1038/onc.2008.123. [PubMed: 18438430]
25. Casey SC, Tong L, Li Y, Do R, Walz S, Fitzgerald KN, et al. MYC regulates the antitumor immune response through CD47 and PD-L1. Science 2016;352(6282):227–31 doi 10.1126/science.aac9935. [PubMed: 26966191]
26. MYC Promotes Tumorigenesis via Activation of CD47 and PD-L1. Cancer Discov 2016;6(5):472 doi 10.1158/2159-8290.CD-RW2016-051.
27. Chatterjee S, Daenthanasanmak A, Chakraborty P, Wyatt MW, Dhar P, Selvam SP, et al. CD38-NAD(+)Axis Regulates Immunotherapeutic Anti-Tumor T Cell Response. Cell Metab 2018;27(1):85–100 e8 doi 10.1016/j.cmet.2017.10.006. [PubMed: 29129787]
28. Royston P, Sauerbrei W. A new measure of prognostic separation in survival data. Statistics in medicine 2004;23(5):723–48 doi 10.1002/sim.1621. [PubMed: 14981672]
29. Chang CH, Pearce EL. Emerging concepts of T cell metabolism as a target of immunotherapy. Nat Immunol 2016;17(4):364–8 doi 10.1038/ni.3415. [PubMed: 27002844]
30. Sena LA, Li S, Jairaman A, Prakriya M, Ezponda T, Hildeman DA, et al. Mitochondria are required for antigen-specific T cell activation through reactive oxygen species signaling. Immunity 2013;38(2):225–36 doi 10.1016/j.immuni.2012.10.020. [PubMed: 23415911]
31. Warfel NA, Sainz AG, Song JH, Kraft AS. PIM Kinase Inhibitors Kill Hypoxic Tumor Cells by Reducing Nrf2 Signaling and Increasing Reactive Oxygen Species. Mol Cancer Ther 2016;15(7):1637–47 doi 10.1158/1535-7163.MCT-15-1018. [PubMed: 27196781]
32. De Rosa V, Galgani M, Porcellini A, Colamatteo A, Santopaolo M, Zuchegna C, et al. Glycolysis controls the induction of human regulatory T cells by modulating the expression of FOXP3 exon 2 splicing variants. Nat Immunol 2015;16(11):1174–84 doi 10.1038/ni.3269. [PubMed: 26414764]
33. Taylor A, Rudd CE. Glycogen Synthase Kinase 3 Inactivation Compensates for the Lack of CD28 in the Priming of CD8(+) Cytotoxic T-Cells: Implications for anti-PD-1 Immunotherapy. Front Immunol 2017;8:1653 doi 10.3389/fimmu.2017.01653. [PubMed: 29312284]
34. Taylor A, Harker JA, Chanthong K, Stevenson PG, Zuniga EI, Rudd CE. Glycogen Synthase Kinase 3 Inactivation Drives T-bet-Mediated Downregulation of Co-receptor PD-1 to Enhance CD8(+) Cytolytic T Cell Responses. Immunity 2016;44(2):274–86 doi 10.1016/j.immuni.2016.01.018. [PubMed: 26885856]
35. Bollum LK, Huse K, Oksvold MP, Bai B, Hilden VI, Forfang L, et al. BMP-7 induces apoptosis in human germinal center B cells and is influenced by TGF-beta receptor type I ALK5. PLoS One 2017;12(5):e0177188 doi 10.1371/journal.pone.0177188. [PubMed: 28489883]
36. Giangreco A, Hoste E, Takai Y, Rosewell I, Watt FM. Epidermal Cadm1 expression promotes autoimmune alopecia via enhanced T cell adhesion and cytotoxicity. J Immunol 2012;188(3):1514–22 doi 10.4049/jimmunol.1003342. [PubMed: 22210910]
37. Mandal M, Borowski C, Palomero T, Ferrando AA, Oberdoerffer P, Meng F, et al. The BCL2A1 gene as a pre-T cell receptor-induced regulator of thymocyte survival. J Exp Med 2005;201(4):603–14 doi 10.1084/jem.20041924. [PubMed: 15728238]

38. Mendel I, Shevach EM. Activated T cells express the OX40 ligand: requirements for induction and costimulatory function. Immunology 2006;117(2):196–204 doi 10.1111/j.1365-2567.2005.02279.x. [PubMed: 16423055]
39. Garre P, Briceno V, Xicola RM, Doyle BJ, de la Hoya M, Sanz J, et al. Analysis of the oxidative damage repair genes NUDT1, OGG1, and MUTYH in patients from mismatch repair proficient HNPCC families (MSS-HNPCC). Clin Cancer Res 2011;17(7):1701–12 doi 10.1158/1078-0432.CCR-10-2491. [PubMed: 21355073]
40. Braso-Maristany F, Filosto S, Catchpole S, Marlow R, Quist J, Francesch-Domenech E, et al. PIM1 kinase regulates cell death, tumor growth and chemotherapy response in triple-negative breast cancer. Nat Med 2016;22(11):1303–13 doi 10.1038/nm.4198. [PubMed: 27775704]
41. Unsoeld H, Pircher H. Complex memory T-cell phenotypes revealed by coexpression of CD62L and CCR7. Journal of virology 2005;79(7):4510–3 doi 10.1128/JVI.79.7.4510-4513.2005. [PubMed: 15767451]
42. Kerdiles YM, Beisner DR, Tinoco R, Dejean AS, Castrillon DH, DePinho RA, et al. Foxo1 links homing and survival of naive T cells by regulating L-selectin, CCR7 and interleukin 7 receptor. Nat Immunol 2009;10(2):176–84 doi 10.1038/ni.1689. [PubMed: 19136962]
43. Fabre S, Carrette F, Chen J, Lang V, Semichon M, Denoyelle C, et al. FOXO1 regulates L-Selectin and a network of human T cell homing molecules downstream of phosphatidylinositol 3-kinase. J Immunol 2008;181(5):2980–9. [PubMed: 18713968]
44. Deng Y, Wang F, Hughes T, Yu J. FOXOs in cancer immunity: Knowns and unknowns. Semin Cancer Biol 2018 doi 10.1016/j.semcancer.2018.01.005.
45. Hedrick SM, Hess Michelini R, Doedens AL, Goldrath AW, Stone EL. FOXO transcription factors throughout T cell biology. Nat Rev Immunol 2012;12(9):649–61 doi 10.1038/nri3278. [PubMed: 22918467]
46. van Elsas A, Hurwitz AA, Allison JP. Combination immunotherapy of B16 melanoma using anti-cytotoxic T lymphocyte-associated antigen 4 (CTLA-4) and granulocyte/macrophage colony-stimulating factor (GM-CSF)-producing vaccines induces rejection of subcutaneous and metastatic tumors accompanied by autoimmune depigmentation. J Exp Med 1999;190(3):355–66. [PubMed: 10430624]
47. Chen S, Lee LF, Fisher TS, Jessen B, Elliott M, Evering W, et al. Combination of 4–1BB agonist and PD-1 antagonist promotes antitumor effector/memory CD8 T cells in a poorly immunogenic tumor model. Cancer Immunol Res 2015;3(2):149–60 doi 10.1158/2326-6066.CIR-14-0118. [PubMed: 25387892]
48. Feldman SA, Assadipour Y, Kriley I, Goff SL, Rosenberg SA. Adoptive Cell Therapy--Tumor-Infiltrating Lymphocytes, T-Cell Receptors, and Chimeric Antigen Receptors. Semin Oncol 2015;42(4):626–39 doi 10.1053/j.seminoncol.2015.05.005. [PubMed: 26320066]
49. Roychoudhuri R, Eil RL, Restifo NP. The interplay of effector and regulatory T cells in cancer. Curr Opin Immunol 2015;33:101–11 doi 10.1016/j.coi.2015.02.003. [PubMed: 25728990]
50. Gurusamy D, Clever D, Eil R, Restifo NP. Novel “Elements” of Immune Suppression within the Tumor Microenvironment. Cancer Immunol Res 2017;5(6):426–33 doi 10.1158/2326-6066.CIR-17-0117. [PubMed: 28576921]
51. Ye Z, Qian Q, Jin H, Qian Q. Cancer vaccine: learning lessons from immune checkpoint inhibitors. J Cancer 2018;9(2):263–8 doi 10.7150/jca.20059. [PubMed: 29344272]
52. Robert L, Ribas A, Hu-Lieskovan S. Combining targeted therapy with immunotherapy. Can 1+1 equal more than 2? Semin Immunol 2016;28(1):73–80 doi 10.1016/j.smim.2016.01.001. [PubMed: 26861544]
53. Nowicki TS, Hu-Lieskovan S, Ribas A. Mechanisms of Resistance to PD-1 and PD-L1 Blockade. Cancer J 2018;24(1):47–53 doi 10.1097/PPO.0000000000000303. [PubMed: 29360728]
54. Swords R, Kelly K, Carew J, Nawrocki S, Mahalingam D, Sarantopoulos J, et al. The Pim kinases: new targets for drug development. Curr Drug Targets 2011;12(14):2059–66. [PubMed: 21777193]
55. Fox CJ, Hammerman PS, Thompson CB. The Pim kinases control rapamycin-resistant T cell survival and activation. J Exp Med 2005;201(2):259–66 doi 10.1084/jem.20042020. [PubMed: 15642745]

56. Kesarwani P, Al-Khami AA, Scurti G, Thyagarajan K, Kaur N, Husain S, et al. Promoting thiol expression increases the durability of antitumor T-cell functions. Cancer Res 2014;74(21):6036–47 doi 10.1158/0008-5472.CAN-14-1084. [PubMed: 25164014]
57. Araki K, Youngblood B, Ahmed R. The role of mTOR in memory CD8 T-cell differentiation. Immunol Rev 2010;235(1):234–43 doi 10.1111/j.0105-2896.2010.00898.x. [PubMed: 20536567]
58. Philip M, Fairchild L, Sun L, Horste EL, Camara S, Shakiba M, et al. Chromatin states define tumour-specific T cell dysfunction and reprogramming. Nature 2017;545(7655):452–6 doi 10.1038/nature22367. [PubMed: 28514453]
59. Amaravadi R, Thompson CB. The survival kinases Akt and Pim as potential pharmacological targets. J Clin Invest 2005;115(10):2618–24 doi 10.1172/JCI26273. [PubMed: 16200194]
60. Warfel NA, Kraft AS. PIM kinase (and Akt) biology and signaling in tumors. Pharmacol Ther 2015;151:41–9 doi 10.1016/j.pharmthera.2015.03.001. [PubMed: 25749412]
61. Tzivion G, Dobson M, Ramakrishnan G. FoxO transcription factors; Regulation by AKT and 14–3-3 proteins. Biochim Biophys Acta 2011;1813(11):1938–45 doi 10.1016/j.bbamcr.2011.06.002. [PubMed: 21708191]
62. Delpoux A, Michelini RH, Verma S, Lai CY, Omilusik KD, Utzschneider DT, et al. Continuous activity of Foxo1 is required to prevent anergy and maintain the memory state of CD8(+) T cells. J Exp Med 2017 doi 10.1084/jem.20170697.
63. Amiel E, Everts B, Freitas TC, King IL, Curtis JD, Pearce EL, et al. Inhibition of mechanistic target of rapamycin promotes dendritic cell activation and enhances therapeutic autologous vaccination in mice. J Immunol 2012;189(5):2151–8 doi 10.4049/jimmunol.1103741. [PubMed: 22826320]
64. Lawless SJ, Kedia-Mehta N, Walls JF, McGarrigle R, Convery O, Sinclair LV, et al. Glucose represses dendritic cell-induced T cell responses. Nat Commun 2017;8:15620 doi 10.1038/ncomms15620. [PubMed: 28555668]
65. Dong G, Wang Y, Xiao W, Pacios Pujado S, Xu F, Tian C, et al. FOXO1 regulates dendritic cell activity through ICAM-1 and CCR7. J Immunol 2015;194(8):3745–55 doi 10.4049/jimmunol.1401754. [PubMed: 25786691]
66. Webb AE, Kundaje A, Brunet A. Characterization of the direct targets of FOXO transcription factors throughout evolution. Aging Cell 2016;15(4):673–85 doi 10.1111/acel.12479. [PubMed: 27061590]
67. Klein Geltink RI, O'Sullivan D, Corrado M, Bremser A, Buck MD, Buescher JM, et al. Mitochondrial Priming by CD28. Cell 2017;171(2):385–97 e11 doi 10.1016/j.cell.2017.08.018. [PubMed: 28919076]
68. Humphrey SJ, James DE, Mann M. Protein Phosphorylation: A Major Switch Mechanism for Metabolic Regulation. Trends Endocrinol Metab 2015;26(12):676–87 doi 10.1016/j.tem.2015.09.013. [PubMed: 26498855]
69. Knudson KM, Pritzl CJ, Saxena V, Altman A, Daniels MA, Teixeiro E. NFkappaB-Pim-1-Eomesodermin axis is critical for maintaining CD8 T-cell memory quality. Proc Natl Acad Sci U S A 2017;114(9):E1659–E67 doi 10.1073/pnas.1608448114. [PubMed: 28193872]
70. Daenthanasanmak A, Wu Y, Iamsawat S, Nguyen HD, Bastian D, Zhang M, et al. PIM-2 protein kinase negatively regulates T cell responses in transplantation and tumor immunity. J Clin Invest 2018 doi 10.1172/JCI95407.

TRANSLATIONAL RELEVANCE

Adoptive T cell immunotherapy studies predominantly comprise of terminally differentiated T cells with effector memory (Tem) phenotype, which have a limited life span. We believe that targeting PIM kinases, which along with Akt phosphorylate overlapping substrates to activate common pathways that control various physiological processes, are important for controlling tumor growth by altering the anti-tumor T cell phenotype. This study shows that PIM inhibition not only leads to increased central memory phenotype of T cells, but it also results in a durable tumor control when used in combination with anti-PD1 antibody. Thus, these studies have high translational potential for tumor immunotherapy protocols being used to treat cancer patients.

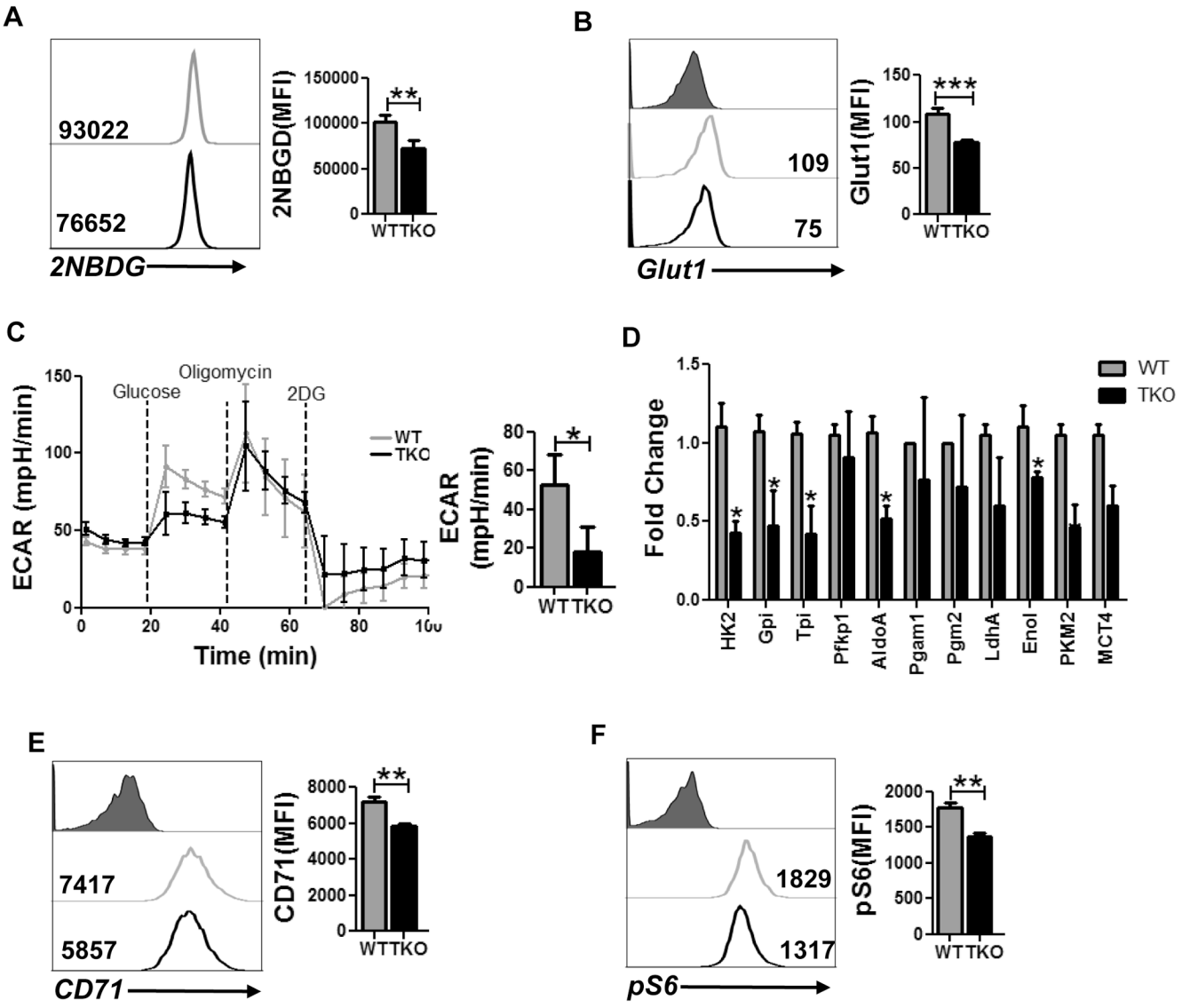

Figure 1. Inhibition of PIM kinases lowers glycolysis in T cells.

Purified CD8 T cells from either WT or TKO mice were activated and used to determine: *A*) 2NBDG uptake, and *B*) cell surface expression of Glut1 using flow cytometry. For *A* & *B*, adjacent bar graph represents the cumulative data of mean fluorescence intensity (MFI) from three independent experiments. *C*) ECAR time course in response to glucose, oligomycin and 2DG (left panel). Adjacent bar graph shows ECAR level after glucose addition. *D*) qPCR analysis of various glycolysis-associated genes in activated T cells from either WT or TKO mice. *E*) Cell surface expression of CD71 using flow cytometry. Adjacent bar diagram represents the cumulative data as MFI from three independent experiments. *F*) Intracellular expression of pS6 in activated T cells. Adjacent bar graph represents the cumulative MFI data from three independent experiments. *p<0.05, **p< 0.01 and ***p<0.005.

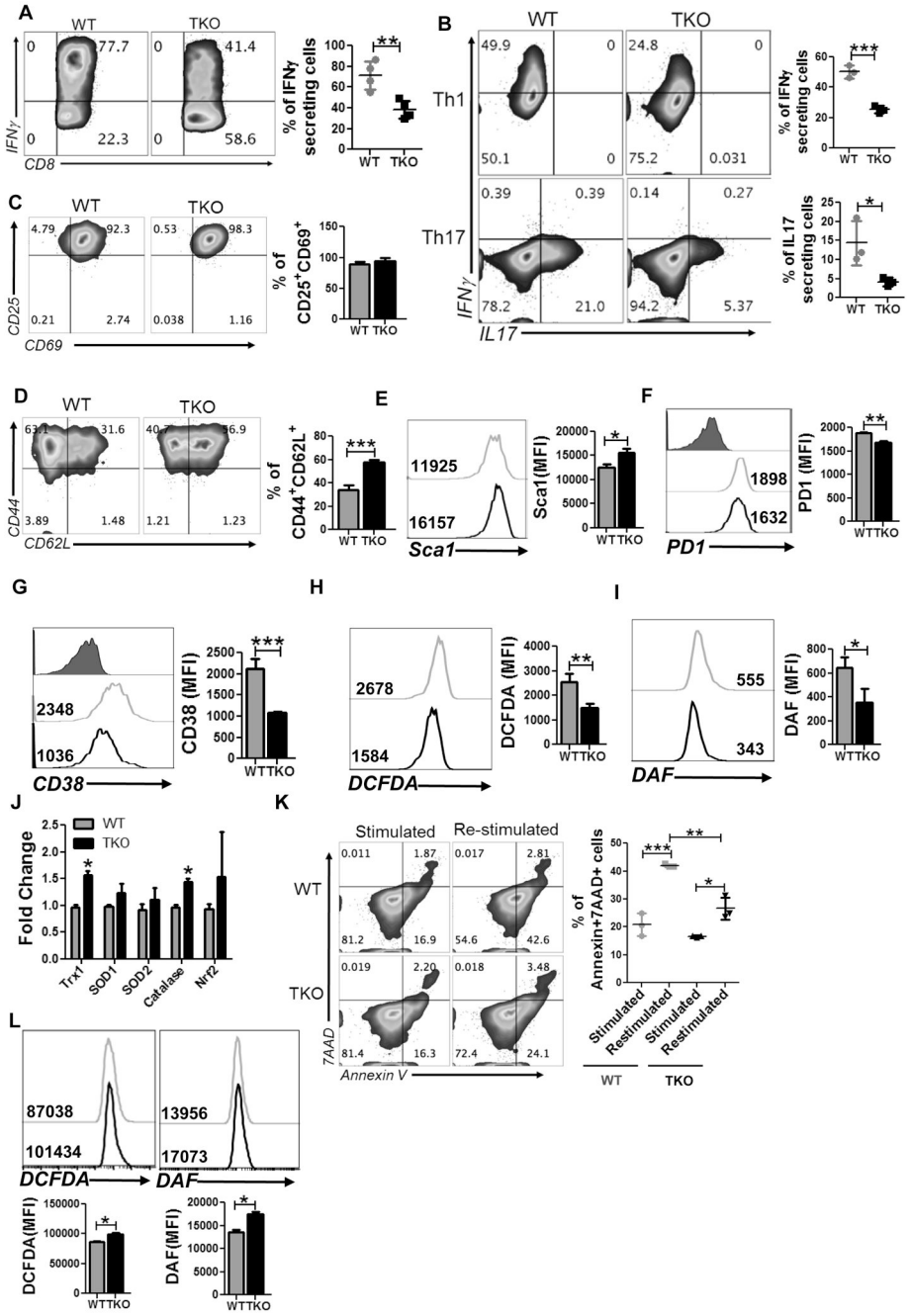

Figure 2. Increased stemness, reduced ROS generation and cell death in TKO T cells.

A-B) Intracellular cytokine secretion by WT and TKO T cells either activated three days in presence of IL2 (*A*), or *in vitro* differentiated Th1 and Th17 cells (*B*). For *A* & *B*, adjacent bar graph represents the cumulative data of MFI from five independent experiments. *C-G*) Cell surface expression of the following on activated WT and TKO T cells: CD25 *vs.* CD69 (*C*), CD44 *vs.* CD62L (*D*), Sca1 (*E*), PD1 (*F*) and CD38 (*G*). For *C-G*, adjacent bar graph represents cumulative MFI data from three independent experiments. *H-I*) Flow cytometric analysis of activated WT and TKO T cells for intracellular ROS level (*H*), and NO level (*I*) measured using DCFDA and DAF respectively. Cumulative MFI data from 3 independent

experiments is represented in the bar graph alongside the histogram. *J*) qPCR analysis of anti-oxidant genes using mRNA obtained from activated T cells. *K*) Activation-induced cell death of WT and TKO T cells was evaluated after overnight re-stimulation with anti-CD3 (2 μg/ml) and anti-CD28 (1 μg/ml). Scatter plot represents the frequency of annexin V^+7AAD^+ CD8 T cells before and after overnight re-stimulation. Data are representative of 3 independent experiment with similar results. *L*) WT and TKO MEF were stimulated with PMA and accumulation of ROS (using DCFDA) and RNS (using DAF) was determined. Cumulative MFI from 3 independent experiments is represented in the bar diagram below the histogram. *p<0.05, **p< 0.01 and ***p<0.005.

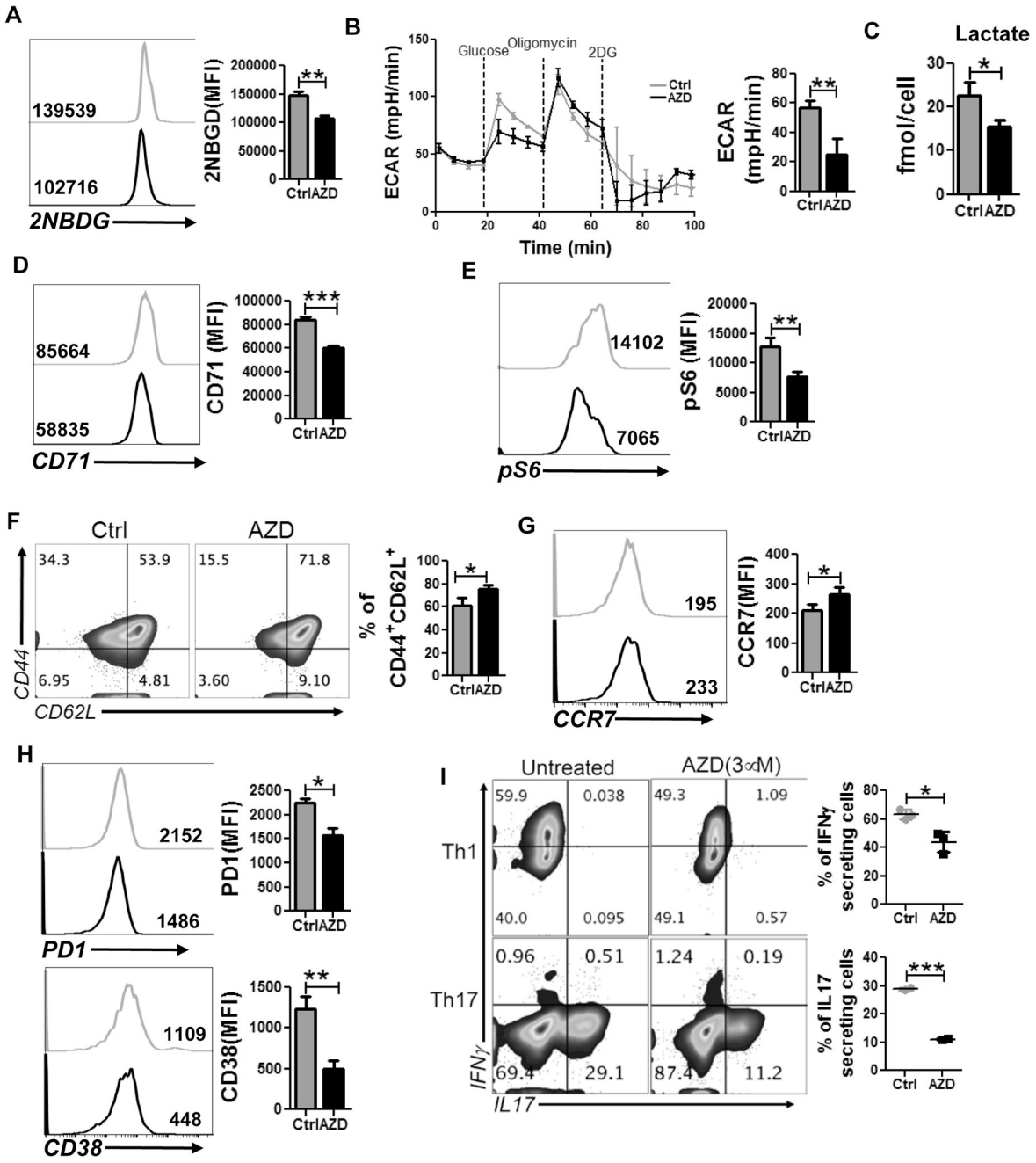

Figure 3. Pan-PIM kinases inhibitor AZD1208 mimics the phenotype observed with TKO T cells.

pMel T cells activated with the cognate antigen either in presence of vehicle control (DMSO) or AZD1208 (3 μM) were used to determine: *A*) uptake of 2NBDG, *B*) ECAR time course following addition of glucose, oligomycin, and 2DG (*left panel*), and ECAR level following addition of glucose (*right panel*), *C*) intracellular level of lactate using NMR, *D*) cell surface expression of CD71, *E*) intracellular expression of pS6, *F*) cell surface expression of CD44 and CD62L, *G*) CCR7, and *H*) PD1 (*upper panel*), and CD38 (*lower panel*). For panel A-H, the bar graph represents the cumulative MFI data from three independent experiments. *I*) intracellular cytokine production by Th1 or Th17 cells

differentiated *in vitro* either in presence or absence of AZD1208 (3 μM). The adjacent scatter plot represents the cumulative data of MFI from there independent experiments. *p<0.05, **p< 0.01 and ***p<0.005.

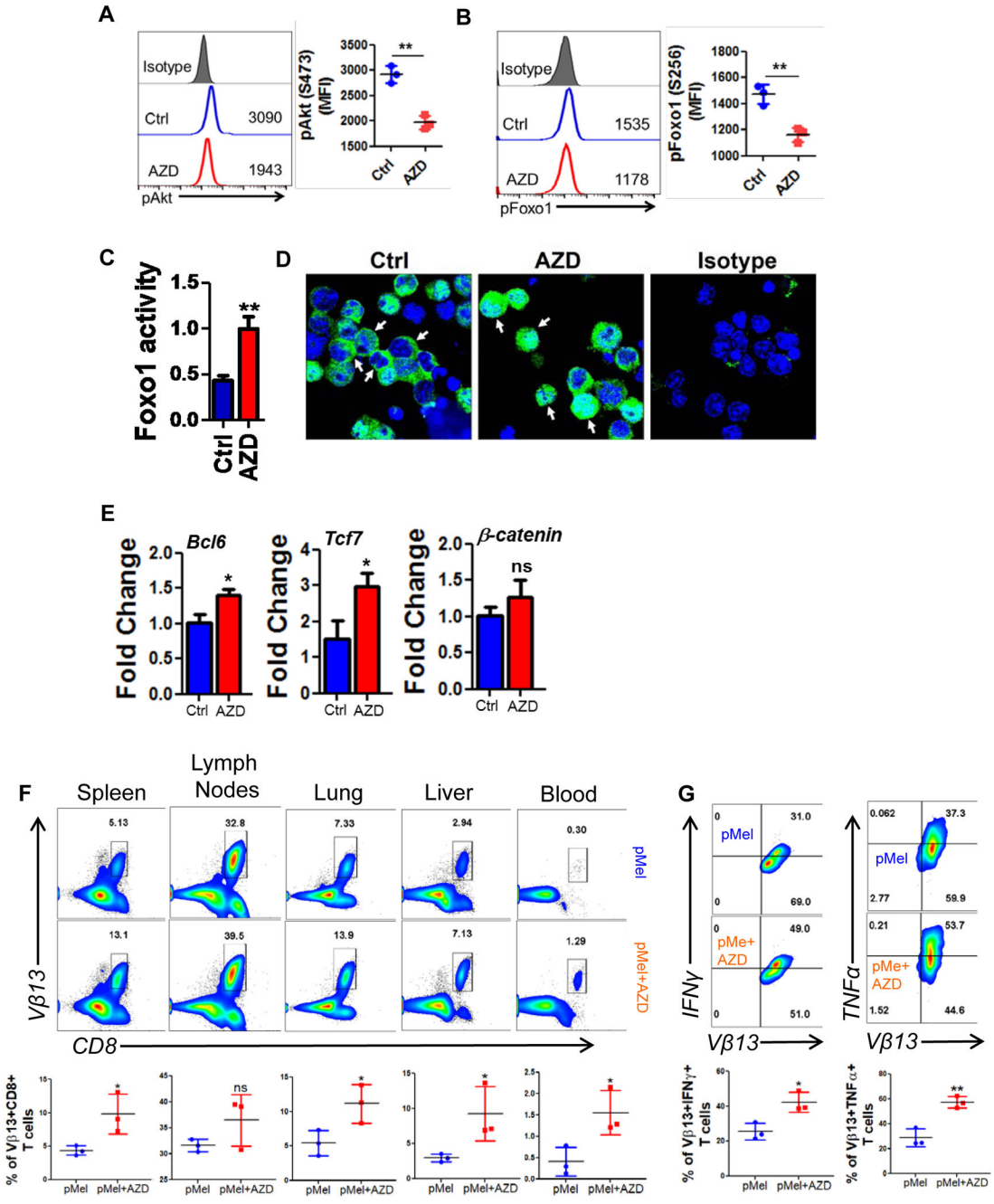

Figure 4. PIM inhibition decreases pAkt and pFoxo1 in T cells.

pMel T cells were activated with the cognate antigen either in presence of vehicle control (DMSO) or AZD1208 (3 μM) before flow cytometry analysis of: *A*) phosphorylated Akt (S473), *B*) phosphorylated Foxo1 (S256), and *C*) ELISA-based determination of Foxo1 activity. For panel *A* & *B*, the adjacent bar graph represents the cumulative mean fluorescence intensity (MFI) data from three independent experiments; panel *C* shows representative data from one of three independent experiments. *D*) Confocal microscopy-based localization of total Foxo1 (green) is shown. DAPI (blue) was used to stain the nucleus. *E*) qPCR analysis of various memory-associated genes in vehicle- or AZD1208-

treated T cells. Average of three independent experiments is shown. *F*) Three day activated pMel or AZD1208 treated pMel transgenic T cells (1×10^6 cells/mouse) were adoptively transferred into $Rag1^{-/-}$ mice. After 25 days of T cell transferred mice were sub-cutaneously injected with B16-F10 solid tumors (0.25×10^6 cells/mouse). *Upper panel* shows representative flow cytometric analysis done to determine the percentage of TCR transgenic T cells retrieved from spleen, lymph nodes, blood, lung, liver after 5 days of tumor injection. *Lower panel* is the cumulative data from different mice. *G*) Splenocytes from (*F*) were stimulated overnight with hgp100 antigen before being analyzed for intracellular signature of IFNγ and TNFα. *N*=3. **p*<0.05, ***p*<0.005, ***p<0.0005.

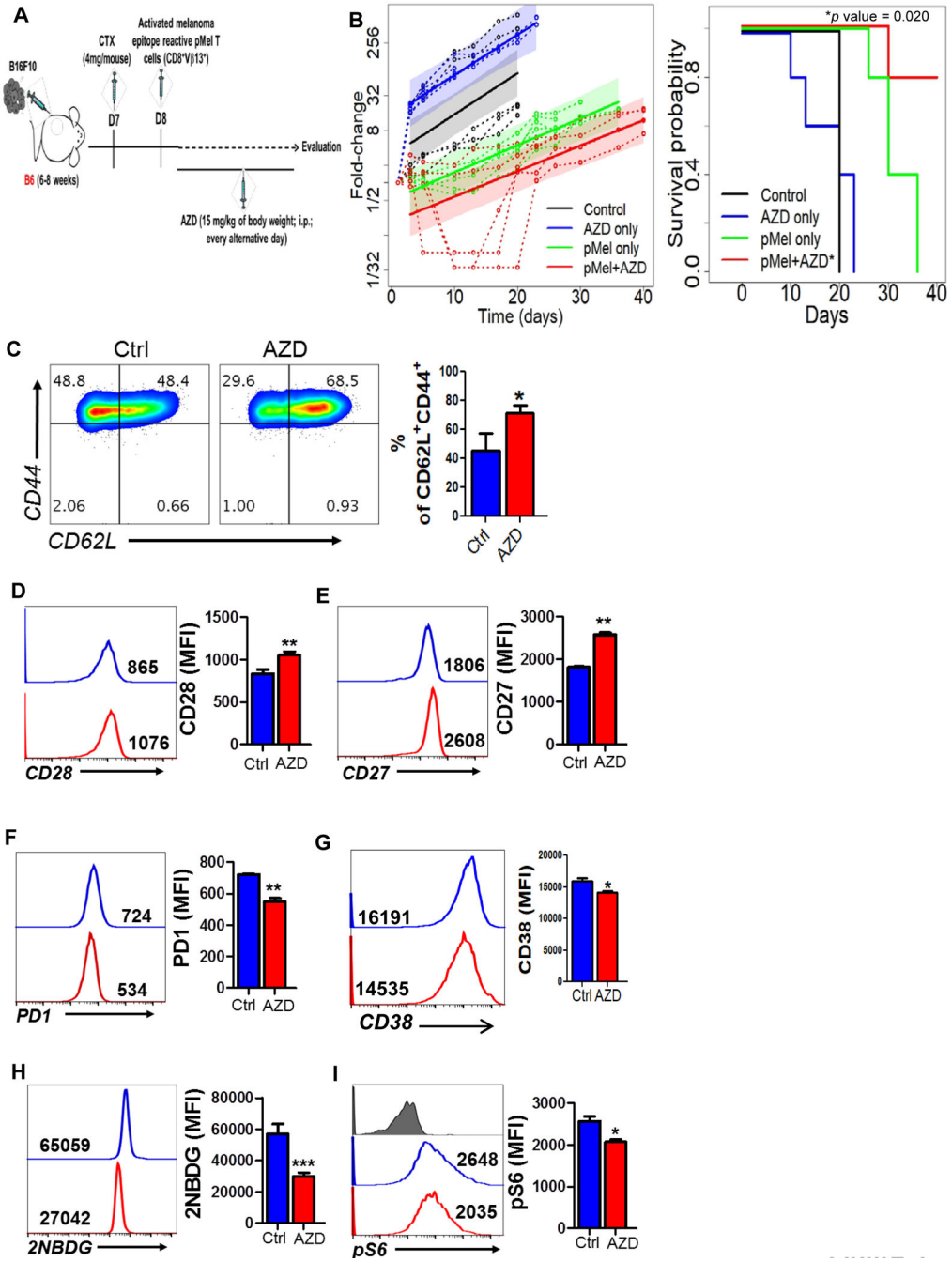

Figure 5. Inhibition of PIM kinases improves the anti-tumor response of T cells.

A) B6 mice (n=5 mice/group) were inoculated via subcutaneous route (*s.c.*) with 0.25 × 10^6 B16-F10 murine melanoma cells and after eight days mice were either injected (*i.p*) with vehicle control (methyl acetate) or AZD1208 or adoptively transferred with three-day-activated pMel T cells (1×10^6 cells/mouse). Mice that received pMel T cells were further subdivided in two groups and either injected (*i.p*) with vehicle (methyl acetate) or AZD1208. Mice were given AZD1208 every other day until day 21. Tumor growth was measured using digital calipers in two dimensions (area (mm^2) = length (mm) × breadth (mm)), every three

days. Schematic diagram (*A*) and fold-change (tumor size relative to tumor size at baseline) over time for each experimental condition is shown (*B*). Fold-change (tumor size relative to tumor size at baseline) over time for each experimental condition. Dashed lines are individual mouse trajectories, solid lines are fitted growth curves based on linear mixed effects regression model (see methods), and shaded regions are point wise 95% confidence regions. *B*) Kaplan-Meier curves for time-to-sacrifice across experimental conditions are shown. Curves have been shifted slightly to facilitate visualization. Comparisons between conditions based on a log-rank test (pMel only versus pMel + AZD, **p value* = 0.020). *C-I*) Human T cells from the healthy donors were activated either in presence of absence of AZD1208 before determining: cell surface expression of CD44 and CD62L (*C*), CD28 (*D*), CD27 (*E*), PD1 (*F*), CD38 (*G*), uptake of 2NBDG (*H*), and phosphorylation of S6 (pS6; *I*). For panels *C-I*, the adjacent bar graph represents the cumulative MFI data from three independent experiments. **p*<0.05, ***p*< 0.01, ****p*<0.005 and **** p < 0.001.

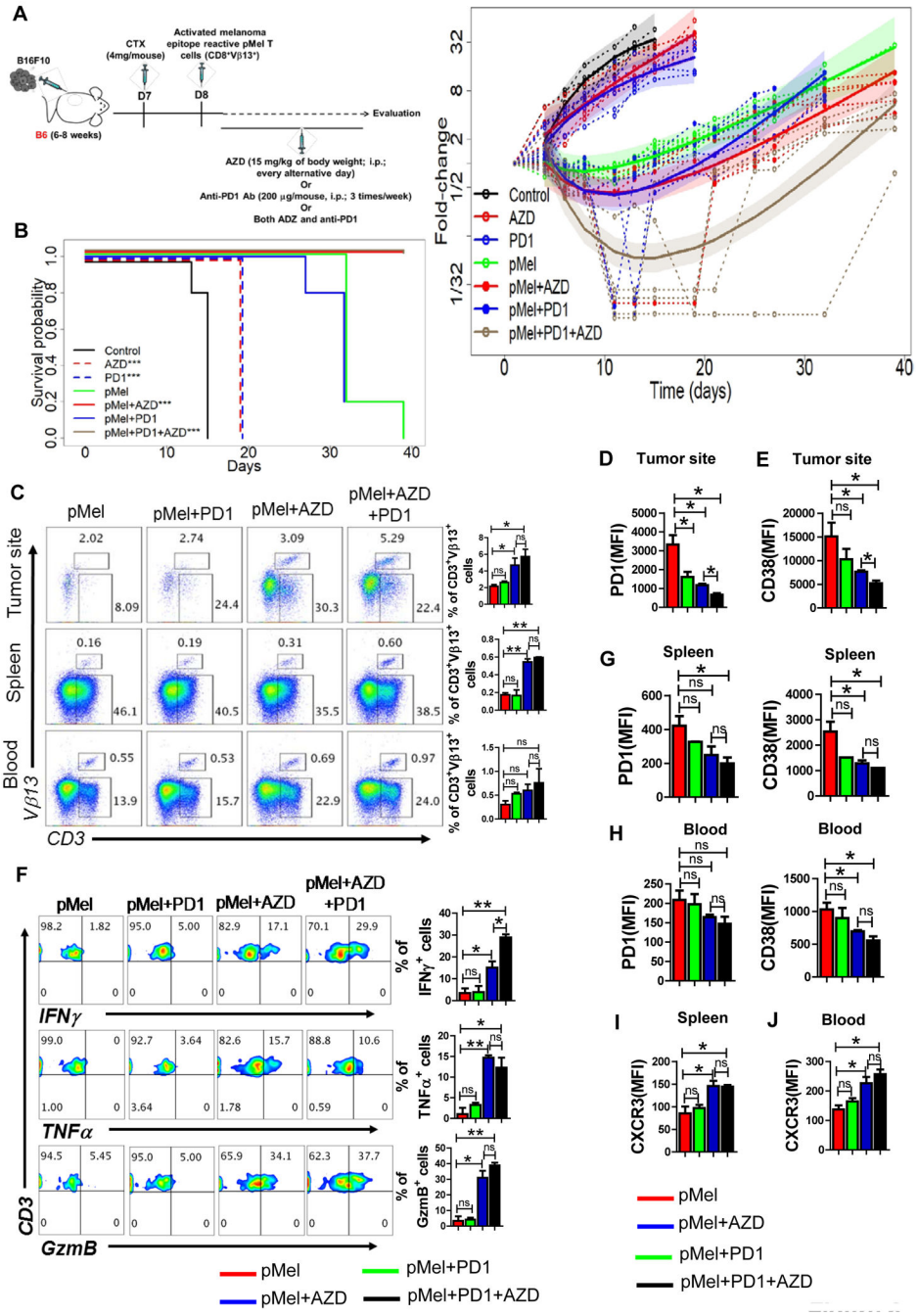

Figure 6. Combination of anti-PD1 with AZD1208 further improves ACT.

A) Experimental scheme showing that C57BL/6 mice (n=5 mice/group) were inoculated via subcutaneous route (*s.c.*) with 0.25×10^6 B16-F10 murine melanoma cells and after eight days mice either injected via intraperitoneal route (*i.p*) with vehicle (methyl acetate) or AZD1208 or adoptively transferred with three-day-activated pMel T cells (1×10^6 cells/ mouse). Cohorts that received pMel T cells were further subdivided in two groups and either injected (i.p) with vehicle (methyl acetate) or AZD1208. Both AZD1208 and anti-PD1 Ab were given every other day until day 21. Tumor growth was measured in two dimensions

(area (mm^2) = length (mm) × breadth (mm)), using digital callipers every three days. *Right panel* shows fold-change (tumor size relative to tumor size at baseline) over time for each experimental condition. Dashed lines are individual mouse trajectories, solid lines are fitted growth curves based on linear mixed effects regression model (see text), and shaded regions are point wise 95% confidence regions. *B*) Kaplan-Meier curves for time-to-sacrifice across experimental conditions are shown. Curves have been shifted slightly to facilitate visualization. Comparisons relative to control based on log-rank tests (control vs. AZD, p = 0.0035; control vs. PD1, p = 0.0035; pMel vs. pMel + AZD, p = 0.0016; pMel vs. pMel + PD1 + AZD, p = 0.0016). *C*) Frequency of adoptively transferred pMel T cells ($V\beta13^+CD3^+$) present at the tumor site, in spleen, and in blood of the tumor-bearing mice 30 days following ACT. Aadjacent bar graph represents the cumulative data of frequency of $V\beta13^+CD3^+$ cells from three excremental mice. Tumor-infiltrating T cells retrieved from the tumor-bearing mice on day 30 were used to determine either surface expression of PD1 (*D*) and CD38 (*E*) or were activated *in vitro* with PMA and ionomycin and assessed for intercellular IFNγ, TNFα and GzmB production using flow cytometry (*F*). For *F*, the adjacent bar graph represents the cumulative data of frequency of cytokine secreting cells from three excremental mice. *G-J*) Bar diagrams represent the cumulative data of MFI of the cell surface expression of either PD1 and CD38 or CXCR3 on the adoptively transferred $V\beta13^+CD3^+$ T cells present either in the spleen (*G* and *I*) or blood (*H* and *J*) of tumor-bearing mice. *p<0.05, **p< 0.01, ***p<0.005 and **** p < 0.001.